Liquefaction Dynamics of *n*-Octadecane in Cylindrical Coordinates

R. L. BAIN,* F. J. STERMOLE,† AND J. O. GOLDEN‡
Colorado School of Mines, Golden, Colo.

The study presents one method of mathematically modeling the effects of gravity-induced free convection upon the melting phenomena of a finite paraffin slab. The theoretical model is based on the numerical computer solution of the solid phase and liquid phase energy equations, coupled with an imposed ideal-viscous flow approximation. An implicit alternating-direction technique is used as the finite-difference approximation for the basic energy equations in the numerical solution. The theoretical predictions are compared to experimental data from an annular test cell, in which *n*-octadecane, $C_{18}H_{38}$, was used as the test material. The results show that the model is a good first approximation to the solution of solid-liquid phase change involving gravity-induced free convection.

Nomenclature

c_{pl} = liquid-phase heat capacity, w · sec/g°K
c_{ps} = solid-phase heat capacity, w · sec/g°K
d_z = radial position of solid-liquid interface for any given vertical position, cm
ΔH_f = latent heat of fusion, w · sec/g
k_l = liquid-phase thermal conductivity, w/cm°K
k_s = solid-phase thermal conductivity, w/cm°K
L = length of cell in vertical direction, cm
q = heat flux, w/cm^2
r = radial spatial coordinate, cm
Δr = radial spatial increment, cm
R_{max} = maximum radial position, cm
R_{min} = minimum radial position, cm
Δt = time increment, sec
T = temperature, °K
T_{df} = phase-change temperature range, °K
T_e = excess degrees, °K
T_{fo} = temperature at which melting begins, °K
T_p = hot wall temperature, °K
u = z component of velocity, cm/sec
v = r component of velocity, cm/sec
z = vertical spatial coordinate, cm
Δz = vertical spatial increment, cm
α = thermal diffusivity, cm^2/sec
η = dimensionless position, p. 300 of Ref. 23
ρ_l = liquid-phase density, g/cm^3
ρ_s = solid-phase density, g/cm^3
ψ = stream function, cm^2/sec

Introduction

PHASE change materials (PCM) have properties which allow them to absorb or release large quantities of energy without appreciable change in temperature. Because of this unique capability PCM thermal control techniques have received increasing attention for spacecraft thermal design.[1-7] While the major emphasis of PCM work has been in the areas of theoretical and empirical research, PCM flight systems have been used in the Lunar Rover and were scheduled for use in Skylab. Because of inherent advantages of simplicity and reliability, a passive solid-liquid PCM can be used in the walls of spacecraft as packaging around electronic equipment to maintain constant temperature of the equipment by absorbing or releasing energy. However, the PCM system is limited by the heat rejection or absorption capacity of the PCM used; this capacity may be affected by many phenomena, such as gravity, surface tension, electricity, and magnetism. The goal of this study was to investigate the effect of gravity-induced free convection upon the liquefaction dynamics of a PCM, and thereby contribute to the understanding of the phase-change process for future use in the design of PCM thermal control packages.

An earlier study was made by Pujado, Stermole, and Golden,[8] using a variable-space-network finite-difference approach, as first proposed by Murray and Landis,[9] to solve two-phase, unidimensional heat conduction equations with a moving interface. Good agreement was obtained between theoretical and experimental results. Another study was performed by Ukanwa, Stermole, and Golden,[10] concerning the solidification of a finite amount of liquid paraffin. A unidimensional, variable-space-network model was established for the solidification of the paraffin, based on the numerical solution by computer of the two-phase, heat conduction equations with moving interface and variable boundary conditions. The model neglected convection, super-cooling effects, and nucleation effects. Good agreement was obtained between theory and data, although the numerical results indicated a faster rate of solidification than observed experimentally.

A study by Shah[11] investigated solid-liquid phase change using microphotographic pictures and thermal response data as experimental analysis tools. A two-dimensional mathematical model was developed for temperature response of the test material and for the average interfacial velocity. An approximate solution, as given by Dusinberre,[12] was used to calculate the phase-change enthalpy increase. Comparison of the results obtained from the theoretical model and experimental data showed reasonably good agreement.

Other phase-change studies have been made by Grodzka and Fan,[13] Chi-Tien and Yin-Chao Yin,[14] Goodman and Shea,[15] Rathjen and Latif,[16] and Budhia and Krieth.[17]

Wilkes and Churchill[18] performed a theoretical study of temperatures in a closed rectangular system under the influence of gravity-induced free convection. The model was developed from the basic equations of motion, energy, and continuity; the assumption of two-dimensional flow precluded the study of turbulent flow. The system of equations was solved by an implicit alternating-direction technique developed by Peaceman

Received September 4, 1973; revision received November 15, 1973. This work was performed as a part of NASA Research Contract NAS8-30511, Mod. 2, Space Sciences Laboratory, Marshall Space Flight Center, Huntsville, Ala.

Index categories: Spacecraft Temperature Control Systems; Heat Conduction; Liquid and Solid Thermophysical Properties.

* Graduate Student, Chemical and Petroleum-Refining Engineering Department; now Chemical Engineer with Garrett Research and Development, La Verne, Calif.

† Director of Research Development and Professor of Chemical and Petroleum-Refining Engineering.

‡ Associate Professor, Chemical and Petroleum-Refining Engineering Department.

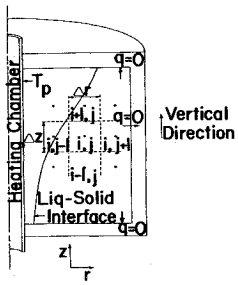

Fig. 1 Theoretical nodal system and boundary conditions.

and Rachford.[19] Instabilities in the numerical solution were observed above certain Grashoff numbers.

Boger and Westwater[20] used the Murray and Landis approach to include the effect of natural convection upon the phase-change process. An effective thermal conductivity, based upon the Nusselt number, was used to successfully model experimental data. The solid-liquid interface was assumed to be flat; in the study being presented here the solid-liquid interface was not flat and this approach could not be used.

An earlier study[21] performed at the Colorado School of Mines dealt with the problem of gravity-induced free convection in the melting of a finite paraffin slab with cartesian geometry. An ideal-viscous flow model was assumed to model the flow pattern; this flow model was coupled with the energy equations, in finite-difference form, to give a theoretical solution. Problems were encountered in reproducibility of experimental data, because of the presence of air bubbles in the test material. Because of these problems it was difficult to be certain that the theoretical solution was modeling the phase-change phenomena accurately.

Theory

In this study a cylindrical-coordinate finite-difference model is developed to predict the transient temperature response of a phase-change material to a step change in one boundary temperature. The model presents one method of calculating the effect of gravity-induced free convection upon the phase-change process.

The test material used in the study was *n*-octadecane, $C_{18}H_{38}$. The following literature values for physical properties were taken from an earlier study[2]: $\rho_s = (-0.8336\times10^{-3})T + 1.0918$ g/cc; $\rho_l = (-0.12505\times10^{-2})T + 1.1316$ g/cc; $c_{ps} = 2.164$ w·sec/g°K; $c_{pl} = (0.8213\times10^{-2})T - 0.14237$ w·sec/g°K; $k_s = (-0.50054\times10^{-5})T + 0.002914$ w/cm°K; $k_l = (-0.50054\times10^{-5})T + 0.002914$ w/cm°K; melting point $\simeq 300.61$°K; liquefaction enthalpy = 243.89 w·sec/g. A diagram of the nodal system and boundary conditions is given by Fig. 1.

The basic energy equations and boundary conditions governing the solid and liquid phases are given below.

Solid phase:

$$\frac{\partial T_s}{\partial t} = \alpha_s\left(\frac{\partial^2 T_s}{\partial z^2} + \frac{1}{r}\frac{\partial T_s}{\partial r} + \frac{\partial^2 T_s}{\partial r^2}\right) \tag{1}$$

Liquid phase:

$$\frac{\partial T_l}{\partial t} + u\frac{\partial T_l}{\partial z} + v\frac{\partial T_l}{\partial r} = \alpha_l\left(\frac{\partial^2 T_l}{\partial z^2} + \frac{1}{r}\frac{\partial T_l}{\partial r} + \frac{\partial^2 T}{\partial r^2}\right) \tag{2}$$

Boundary conditions:

$z = 0,\quad q_z = 0,\quad u(0,j) = v(0,j) = 0$

$z = L,\quad q_z = 0,\quad u(1,j) = v(1,j) = 0$

$r = R_{\min},\quad T(r,z,t) = T_p,\quad u(i,R_{\min}) = v(i,R_{\min}) = 0$

$r = d_z,\quad T(r,z,t) = T_f,\quad u(i,d_z) = v(i,d_z) = 0$

$r = R_{\max},\quad q_r = 0$

Because of the small node size needed in the finite-difference solution, an implicit method of solution is developed. An implicit alternating-direction technique has been developed[19] which is inherently stable with respect to time and spatial increments. The method involves the use of two successive time steps, each of duration t. During the first time step, the derivatives in the r direction are solved implicitly, and the derivatives in the z direction are solved explicitly. The procedure is reversed for the second time step. Let T^* denote temperatures computed at the end of the first time step, and T° denote temperatures computed at the end of the second time step. The r direction has a j subscript, and the z direction has an i subscript. The solid-phase finite-difference approximations of Eq. (1) are given below. The equations are for interior nodes only; special forms of these equations are needed for boundary nodes.

First time step:

$$A_1T_s^*(i,j-1) + B_1T_s^*(i,j) + C_1T_s^*(i,j+1) = D_1 \tag{3a}$$

where

$$A_1 = -\frac{\alpha_s\Delta t}{\Delta r}\left(\frac{1}{\Delta r} + \frac{1}{2r}\right) \tag{3b}$$

$$B_1 = 1.0 + 2\alpha_s\Delta t/(\Delta r)^2 \tag{3c}$$

$$C_1 = A_1 \tag{3d}$$

$$D_1 = T(i,j) + \frac{\alpha_s\Delta t}{(\Delta z)^2}[T(i+1,j) + T(i-1,j) - 2T(i,j)] \tag{3e}$$

Second time step:

$$A_2T_s^\circ(i-1,j) + B_2T_s^\circ(i,j) + C_2T_s^\circ(i+1,j) = D_2 \tag{4a}$$

where

$$A_2 = -\alpha_s\Delta t/(\Delta z)^2 \tag{4b}$$

$$B_2 = 1.0 + 2\alpha_s\Delta t/(\Delta z)^2 \tag{4c}$$

$$C_2 = A_2 \tag{4d}$$

$$D_2 = [\alpha_s\Delta t/(\Delta r)^2][T^*(i,j+1) + T^*(i,j-1) - 2T^*(i,j)] + T^*(i,j) + (\alpha_s\Delta t/2r\Delta r)[T^*(i,j+1) - T^*(i,j-1)] \tag{4e}$$

The liquid-phase finite-difference approximations of Eq. (2) for interior nodes are given below.

First time step:

$$A_3T_l^*(i,j-1) + B_3T_l^*(i,j) + C_3T_l^*(i,j+1) = D_3 \tag{5a}$$

where

$$A_3 = \frac{\Delta t}{\Delta r}\left(-\frac{v(i,j)}{2} - \frac{\alpha_l}{\Delta r} - \frac{\alpha_l}{2r}\right) \tag{5b}$$

$$B_3 = 1.0 + 2\alpha_l\Delta t/(\Delta r)^2 \tag{5c}$$

$$C_3 = \frac{\Delta t}{\Delta r}\left(\frac{v(i,j)}{2} - \frac{\alpha_l}{\Delta r} - \frac{\alpha_l}{2r}\right) \tag{5d}$$

$$D_3 = T(i,j) + \frac{\Delta t u(i,j)}{2\Delta z}[T(i-1,j) - T(i+1,j)] + \frac{\Delta t\alpha_l}{(\Delta z)^2}[T(i+1,j) + T(i-1,j) - 2T(i,j)] \tag{5e}$$

Second time step:

$$A_4T_l^\circ(i-1,j) + B_4T_l^\circ(i,j) + C_4T_l^\circ(i+1,j) = D_4 \tag{6a}$$

where

$$A_4 = \frac{\Delta t}{\Delta z}\left(-\frac{u(i,j)}{2} - \frac{\alpha_l}{\Delta z}\right) \tag{6b}$$

$$B_4 = 1.0 - 2\alpha_l\Delta t/(\Delta z)^2 \tag{6c}$$

$$C_4 = \frac{\Delta t}{\Delta z}\left(\frac{u(i,j)}{2} - \frac{\alpha_l}{\Delta z}\right) \tag{6d}$$

$$D_4 = T^*(i,j) + \frac{u(i,j)\Delta t}{2\Delta r}[T^*(i,j-1) - T^*(i,j+1)] + \frac{\alpha_l\Delta t}{(\Delta r)^2}[T^*(i,j+1) + T^*(i,j-1) - 2T^*(i,j)] + \frac{\alpha_l\Delta t}{2r\Delta r}[T^*(i,j+1) - T^*(i,j-1)] \tag{6e}$$

The temperature equations are solved using a tridiagonal-matrix recursion technique. Given a set of simultaneous equations of the following form:

$$\begin{aligned} b_2 s_2 + c_2 s_3 &= d_2 \\ a_3 s_2 + b_3 s_3 + c_3 s_4 &= d_3 \\ \cdots &= \cdots \\ a_{m-2} s_{m-3} + b_{m-2} s_{m-2} + c_{m-2} s_{m-1} &= d_{m-2} \\ a_{m-1} s_{m-2} + b_{m-1} s_{m-1} &= d_{m-1} \end{aligned} \tag{7}$$

where s_j = unknown temperature at node (i,j). The matrix of the coefficients is a tridiagonal matrix, and is solved using the following equations:

$$\begin{aligned} s_{m-1} &= g_{m-1} \\ s_k &= g_k - f_k s_{k+1}, \quad \text{for} \quad k = m-2, m-3, \ldots, 3, 2 \end{aligned} \tag{8}$$

where the g's and f's are determined by the recursion formulas

$$\begin{aligned} w_2 &= b_2 \\ w_k &= b_k - a_k f_{k-1}, \quad \text{for} \quad k = 3, 4, \ldots, m-2, m-1 \\ f_k &= c_k / w_k, \quad \text{for} \quad k = 2, 3, \ldots, m-2, m-1 \\ g_2 &= d_2 / w_2 \\ g_k &= (d_k - a_k g_{k-1}) / w_k, \quad \text{for} \quad k = 3, 4, \ldots, m-2, m-1 \end{aligned} \tag{9}$$

This regression technique is used to solve both solid and liquid phase energy equations. During the first time step each row, $j = 2$ to $m-1$, is solved by the above technique, going explicitly from $i = 2$ to $n-1$. During the second time step the procedure is reversed, using the appropriate energy equations.

A variation of the method of excess degrees is used for the calculation of the phase-change energy change. Since the *n*-octadecane used in the study was practical grade, not pure material, the assumption is made that the phase change occurs over a temperature range. The procedure for calculating the phase change is given below. After each iteration for the energy equations the phase-change test is made for all solid nodes.

Given:

$$T_s(i,j) \cdot R \cdot T_{fo} \tag{10}$$

If $T_s(i,j) < T_{fo}$, the node is still solid (11)

If $T_s(i,j) \geqq T_{fo}$, the node is changing phase (12)

If Eq. (12) is applicable for the node being investigated then the following procedure is used.

Given:

$$T_e(i,j) = T_s(i,j) - T_{fo} + SUM(i,j) \tag{13}$$

where $SUM(i,j) = \Sigma_t [T(i,j) - T_{fo}]$ for past time steps.

Also given:

$$T_e(i,j) \cdot R \cdot \Delta H_f / c_{ps} \tag{14}$$

If $T_e(i,j) < \Delta H_f / c_{ps}$, the node has not changed phase and the temperature is given by

$$T_s(i,j) = T_{fo} + T_e(i,j) c_{ps} T_{df} / \Delta H_f \tag{15}$$

If $T_e(i,j) \geqq \Delta H_f / c_{ps}$, then the node has changed phase and the liquid-phase temperature is given by

$$T_l(i,j) = T_{fo} + T_{df} + [T_e(i,j) c_{ps} - H_f] / c_{ps} \tag{16}$$

Although the implicit solution developed in this study has eliminated the time-step stability criteria, oscillatory stability criteria still exist which limit the magnitude of allowable velocities, for fixed node size, in the computer solution. The stability criteria for velocities from the finite-difference formulation of Eq. (2) are given below.

$$u \leqq 2\alpha_l / \Delta z \tag{19}$$

$$-v \leqq \alpha_l [r/(\Delta r - 1)], \quad \text{for} \quad v < 0 \tag{20}$$

$$v \leqq \alpha_l [r/(\Delta r + 1)], \quad \text{for} \quad v > 0 \tag{21}$$

The original approach used for velocity profile determination was a modified form of the development proposed by Wilkes and Churchill.[18] Because of relative magnitudes of kinematic viscosity and thermal diffusivity for *n*-octadecane it was found that the oscillatory stability criteria could be satisfied in the vorticity equation, and still not be satisfied in the energy equation. A complex combination of forward and backward, explicit finite differences, in which each node of the liquid phase is evaluated at each time step for the finite-difference formulation which will give a stable solution, is possible. The stability criteria, using either forward or backward differences, of Eq. (2) is given by

$$\frac{2\alpha_l \Delta t}{(\Delta z)^2} + \frac{2\alpha_l \Delta t}{(\Delta r)^2} \leqq 1 \pm \frac{u \Delta t}{\Delta z} \pm \left(\frac{v \Delta t}{\Delta r} - \frac{\alpha_l \Delta t}{r \Delta r} \right) \tag{22}$$

where (+) on velocity term = forward difference in coordinate direction and (−) on velocity term = backward difference in coordinate direction.

In the system being studied both the z and r components of velocity may change sign. By evaluating each node of the liquid phase in terms of positive and negative velocity components, and then choosing the appropriate finite-difference approximation from the various combinations possible in Eq. (22), the following stability criteria can always be satisfied.

$$\Delta t \leqq 1.0 \Big/ \left\{ \frac{2\alpha_l}{(\Delta z)^2} + \frac{2\alpha_l}{(\Delta r)^2} + \frac{\alpha_l}{r \Delta r} \right\} \tag{23}$$

A similar approach can be used to approximate the vorticity equation; and velocity components can then be solved by the approach used in Ref. 18. Because of computer memory and time restrictions it was not possible to develop a solution program using this technique. Therefore, an ideal-viscous flow model has been developed to approximate the flow pattern which exists in the liquid phase. The velocity profile used in the model is an approximate profile obtained by combining an ideal flow system for flow in a cul-de-sac[22] region with a viscous flow solution for flow between parallel plates,[23] see Fig. 2. This combination of flow patterns was chosen to give an approximation to cellular free convection with one roll cell. A maximum velocity is imposed on the flow pattern, using the stability criteria from the liquid phase energy equation. The flow profile for the parallel flow region is

$$v = v_{\max} [(\eta^3 - \eta)/(\eta_o^3 - \eta_o)] \tag{24}$$

where $\eta = r_c/b$ and $\eta_o = \pm 1/(3)^{1/2}$ (from centerline as defined in Fig. 2).

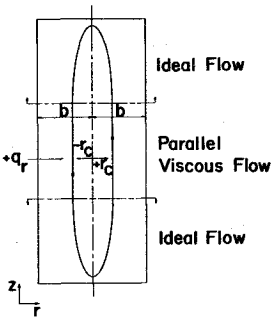

Fig. 2 Liquid phase flow regions and flowfield.

The ideal-flow profiles are developed by the use of complex variable transformations. The basic assumptions made in the conformal transformation process are that 1) the flow pattern being studied is irrotational flow of a perfect fluid, and that 2) the combined flow pattern can be transformed by the use of complex variables into parallel uniform flow. The equations used in the ideal flow model as a result of the conformal transformation process are:

Stream function

$$\psi = -\sinh(\pi z/l) \sin(\pi r/l) \tag{25}$$

Z component of velocity

$$u = -(\pi/l) \sinh(\pi z/l) \cos(\pi r/l) \tag{26}$$

R component of velocity

$$v = (\pi/l) \cosh(\pi x/l) \sin(\pi r/l) \tag{27}$$

The ideal flow regions are coupled to the viscous flow region by assuming the velocities in the viscous flow region are boundary

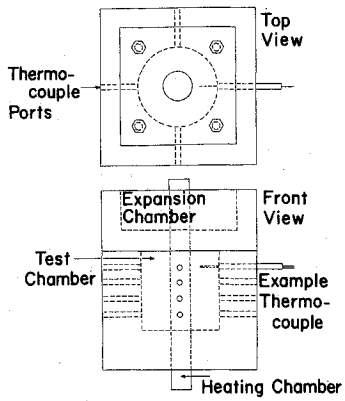

Fig. 3 Test cell diagram.

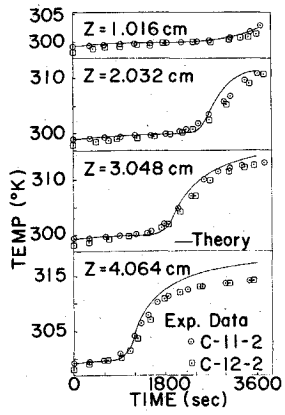

Fig. 5 Comparison of experimental data to theoretical model at $(R-R_{min}) = 0.635$ cm, and $T_p = 321.33$°K.

values for the ideal flow regions. All r-components of velocity are assumed to be zero at this point. The ideal flow regions are imposed at the top and bottom of the liquid phase, and the viscous flow region is imposed in the middle of the liquid phase. By the use of Eq. (25) values of the stream function may be calculated at the ideal-viscous flow boundary. Since there can be no flow across a streamline, velocities in the ideal flow regions can be related to boundary velocities at given values of the stream function at the boundary. By this method a pseudo-viscous flow pattern can be imposed upon the ideal flow regions. The computer program to solve the theoretical model was written in FORTRAN-IV and run on a DEC, Model PDP-10 digital computer.

Experimental Study

The test cell, Fig. 3, consisted of an annular test chamber, a tubular heating chamber, and an expansion chamber. The heating chamber was an aluminum tube with an outside diameter of 1.906 cm. The test chamber was machined in a $10.16 \times 10.16 \times 7.62$-cm block of plexiglas; the expansion chamber, $7.62 \times 7.62 \times 2.54$ cm, was machined from a $10.16 \times 10.16 \times 3.76$-cm block of plexiglas. Sixteen iron-constantan thermocouples, made from 24-gauge wire, were placed in the test chamber at specific radial and vertical positions. Thermocouples were also used to measure the heating tank temperature and the heating wall temperature. The expansion chamber and test chamber were connected using four 0.3175-cm-diam bolts.

The heating system consisted of the following equipment: a constant temperature bath and controller, a centrifugal pump, a flowmeter, and heating fluid flow loop. Temperatures were recorded using a Bristol Dynamaster Multipoint recorder with an accuracy of ±0.417°K. Detailed diagrams of the test cell and equipment system are given in Ref. 24. Six sets of reproduced melting runs and one set of reproduced solidification runs were performed in the experimental study.

Results

Partial results of the study are presented here. Figure 3 shows a sample result from the solidification study used to determine effective thermal properties. In this portion of the study the experimental data from the solidification runs were compared to a unidimensional, finite-difference model using the phase-change calculational procedure previously discussed. It was found that thermal diffusivity could vary by an order of magnitude in the theoretical solution without changing the theoretical predictions. However, the ratio of $\Delta H/c_p$ used in the phase-change calculation had a large effect on the theoretical solution, as shown in Fig. 4. Therefore an effective $\Delta H/c_p$ was used in the theoretical solution of the melting problem. The justifications for this assumption are given below.

1) Since only practical grade n-octadecane was used in the study, the physical properties may be different from literature values.

2) Impurities may have existed in the test material, because of leaching of plasticizers from the plexiglas wall, or because of other forms of contamination.

3) The experimental conditions used in the study were not the same as those used in the determination of physical properties.

Reference 2 states "The apparent major difficulties encountered in the solid density measurements of the normal paraffins were the tendency for the materials either to trap or dissolve air or funnel during solidification.... Despite the painstaking care used in laying down a compact mass of material in the pycnometer, the density values showed a wide variation." Since the physical properties used in this study were based on mass per unit volume, voids or air pockets in the solid would affect the mass of solid in the cell, and thus affect the desired physical properties in the theoretical solution.

Figures 5 and 6 shows partial results from a comparison of experimental data to theoretical prediction for a hot-wall temperature of 321.33°K. In these figures the r position is the distance from the hot wall, and the z position is the distance from the bottom of the cell. The results show the effect of convection; the thermocouples at the larger z positions show a faster melting rate, for example, the melt time in Fig. 4 for $z = 4.064$ cm is

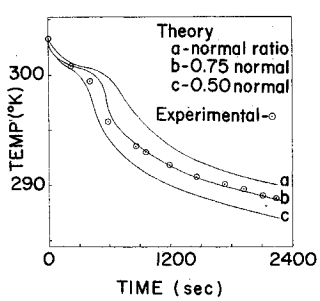

Fig. 4 Comparison of experimental data to theoretical model for a solidification run.

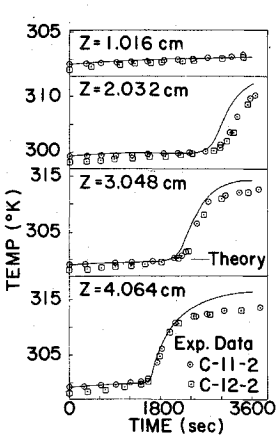

Fig. 6 Comparison of experimental data to theoretical model at $(R-R_{min}) = 0.9525$ cm, and $T_p = 321.33$°K.

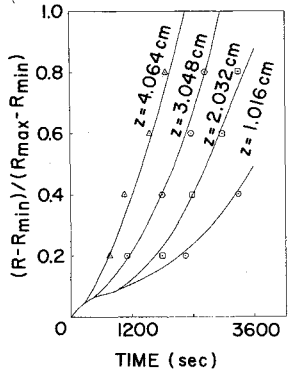

Fig. 7 Effect of convection on solid-liquid interface.

approximately 1000 sec and the melt time for $z = 1.016$ cm is approximately 2600 sec. The theoretical model predicts melting times well; it also predicts the shape of the experimental temperature profiles well. Deviation does occur between final experimental and theoretical temperatures at $z = 4.064$ cm; this is caused by the insulated boundary condition used in the theoretical model not accurately modeling experimental boundary conditions. Because of computer memory restrictions it was not possible to include wall effects in the energy balances developed theoretically.

Figure 7 presents a comparison between experimental interface position and the theoretical interface position for a hot wall temperature of 321.33°K. In this figure the solid lines represent theoretical predictions and the symbols experimental values. The symbols correspond to the following positions: triangles—$z = 4.064$ cm, hexagons—$z = 3.048$ cm, squares—$z = 2.032$ cm, and circles—$z = 1.016$ cm. In all cases there is close agreement between data and theory.

Conclusions

The determination of physical properties is very critical for the proper modeling of the phase-change process. When working with materials with a very low thermal diffusivity, such as *n*-octadecane, the ratio of latent heat to heat capacity becomes the governing factor in the model developed in this study. Therefore, determination of physical properties for the particular experimental system under investigation is needed.

The numerical study assumed that the velocity profiles were symmetric, in magnitude but not direction, in the development of the ideal-viscous flow model. However, experiments were made using a cylindrical geometry test cell. Nodes farther from the tubular heating wall contained more mass than nodes closer to the heating wall; therefore, the flow model should be modified to account for the fact that velocities near the hot wall should be larger in magnitude than in nodes farther from the hot wall. Other sources of numerical error are the constant maximum velocity and the limitation placed on velocity by the oscillatory stability criteria in the liquid-phase energy equation.

A comparison of experimental data and theoretical prediction indicates that the method of solution, an ideal-viscous flow model coupled with the energy equation, will model experimental data when liquid-phase temperature gradients are small. When the liquid-phase temperature gradients become large, deviations appear between final theoretical and experimental temperatures. Therefore, the theoretical solution should be considered as a preliminary solution to the problem of gravity-induced free convection effects in solid-liquid phase-change phenomena.

References

[1] Bannister, T. C. and Bentilla, E. W., "Study on Thermal Control by Use of Fusible Materials," *Proceedings of the Annual Technical Meeting,* Institute of Environment Sciences, San Diego, Calif., 1966, pp. 593–607.

[2] Bentilla, E. W., Stewart, K. F., and Kane, L. E., "Thermal Control by Use of Fusible Materials," Final Report, Contract NAS8-11163, April 1966, Northrup Space Labs., Hawthorne, Calif.

[3] Bain, R. L., Stermole, F. J., and Golden, J. O., "Gravity-Induced Free Convection Effects in Melting Phenomena for Thermal Control," *Journal of Spacecraft and Rockets,* Vol. 8, No. 9, Sept. 1971, pp. 1000–1002.

[4] Hale, D. V., Hoover, M. J., and O'Neill, M. J., "Phase Change Materials Handbook," Contract NASA CR-61363, 1971, Lockheed Missiles and Space Co., Huntsville, Ala.

[5] Young, C. T. K., Harper, T. D., and Ingram, E. H., "PCM-Heat Transfer Improvement Study," Contract NAS8-28576, 1973, Teledyne Brown Engineering, Huntsville, Ala.

[6] Golden, J. O. and Scheldon, B. G., "Development of a Phase Change Thermal Control Device," AIAA Paper 72-287, San Antonio, Texas, 1972.

[7] Golden, J. O. and Scheldon, B. G., "Development of a Phase Change Thermal Control Device," *Journal of Spacecraft and Rockets,* Vol. 10, No. 2, Feb. 1973, pp. 99–100.

[8] Pujado, P. R., Stermole, F. J., and Golden, J. O., "Melting of a Finite Paraffin Slab as Applied to Phase-Change Thermal Control," *Journal of Spacecraft and Rockets,* Vol. 6, No. 3, March 1969, pp. 280–284.

[9] Murray, W. D. and Landis, F., "Numerical and Machine Solutions of Transient Heat-Conduction Problems Involving Melting or Freezing," *Transactions of the ASME: Journal of Heat Transfer,* Ser. C, Vol. 81, No. 2, 1959, pp. 106–112.

[10] Ukanwa, A. O., Stermole, F. J., and Golden, J. O., "Phase Change Solidification Dynamics," *Journal of Spacecraft and Rockets,* Vol. 8, No. 2, Feb. 1971, pp. 193–196.

[11] Shah, A. P., "A Microscopic and Thermal Study of the Solidification of N-octadecane," Thesis T-1334, 1970, Colorado School of Mines, Golden, Colo.

[12] Dusinberre, G. M., *Heat-Transfer Calculations by Finite Differences,* International Textbook Corp., Scranton, Pennsylvania, 1961, Chap. 11.

[13] Grodzka, P. G. and Fan, C., "Thermal Control by Melting and Freezing—Space Thermal Control Study," Interim Report, Contract NAS8-21133, March 1968, Lockheed Missiles and Space Co., Huntsville, Ala.

[14] Chi-Tien and Yin-Chao Yen, "Approximate Solution of a Melting Problem with Natural Convection," *Chemical Engineering Progress Symposium Series,* Vol. 62, No. 64, 1966, pp. 166–172.

[15] Goodman, T. R. and Shea, J. J., "The Melting of Finite Slabs," *Transactions of the ASME: Journal of Applied Mechanics,* Feb. 1960, pp. 16–24.

[16] Rathjen, K. A. and Jiji, L. M., "Heat Conduction with Melting or Freezing in a Corner," *Transactions of the ASME: Journal of Heat Transfer,* Vol. 93, No. 1, 1971, pp. 101–109.

[17] Budhia, H. and Kreith, F., "Heat Transfer with Melting or Freezing in a Wedge," *International Journal of Heat and Mass Transfer,* Vol. 16, No. 1, 1973, pp. 195–200.

[18] Wilkes, J. O. and Churchill, S. W., "The Finite-Difference Computation of Natural Convection in a Rectangular Enclosure," *AIChE Journal,* Vol. 12, No. 1, Jan. 1966, pp. 161–166.

[19] Peaceman, D. W. and Rachford, H. H., "The Numerical Solution of Parabolic and Elliptic Differential Equations," *Journal of the Society for Industrial and Applied Mathematics,* Vol. 3, No. 1, March 1955, pp. 28–41.

[20] Boger, D. V. and Westwater, J. W., "Effect of Buoyancy on the Melting and Freezing Process," *Transactions of the ASME: Journal of Heat Transfer,* Ser. C, Vol. 89, No. 1, Feb. 1967, pp. 81–89.

[21] Bain, R. L., Stermole, F. J., and Golden, J. O., "The Effect of Gravity-Induced Free Convection Upon the Melting Phenomena of a Finite Paraffin Slab for Thermal Control," Annual Summary Report 1, Contract NAS8-30511, Mod. 1, Jan. 1972, Colorado School of Mines, Golden, Colo.

[22] Vallentine, H. R., *Applied Hydrodynamics,* Butterworth, London, England, 1959, Chaps. 5 and 6.

[23] Bird, R. B., Stewart, W. E., and Lightfoot, E. N., *Transport Phenomena,* Wiley, New York, 1960, Chap. 9.

[24] Bain, R. L., "An Experimental and Theoretical Investigation of the Liquefaction Dynamics of a Phase-Change Material in a Normal Gravity Environment," Thesis T-1542, 1973, Colorado School of Mines, Golden, Colo.